Osmolarity Effects on Red Blood Cell Elution in Sedimentation Field-Flow Fractionation

N. Emmanuel Assidjo[1], **Thierry Chianéa**[2], **Igor Clarot**[1], **Marie F. Dreyfuss**[1], and **Philippe J.P. Cardot**[1,*]

[1]Laboratoire de Chimie Analytique et Bromatologie, Université de Limoges, Faculté de Pharmacie, 2 rue du Docteur Marcland, 87025 Limoges Cedex, France and [2]Laboratoire de Biophysique, Université de Limoges, Faculté de Médecine, 2 rue du Docteur Marcland, 87025 Limoges Cedex, France

Abstract

Field-flow fractionation (FFF) is an analytical technique particularly suitable for the separation, isolation, and characterization of macromolecules and micrometer- or submicrometer-sized particles. This chromatographic-like methodology can modulate the retention of micron-sized species according to an elution mode described to date as "steric hyperlayer". In such a model, differences in sample species size, density, or other physical parameters make particle selective elution possible depending on the configuration and the operating conditions of the FFF system. Elution characteristics of micron-sized particles of biological origin, such as cells, can be modified using media and carrier phases of different osmolarities. In these media, a cells average size, density, and shape are modified. Therefore, systematic studies of a single reference cell population, red blood cells (RBCs), are performed with 2 sedimentation FFF systems using either gravity (GrFFF) or a centrifugational field (SdFFF). However, in all cases, normal erythrocyte in isotonic suspension elutes as a single peak when fractionated in these systems. With carrier phases of different osmolarities, FFF elution characteristics of RBCs are modified. Retention modifications are qualitatively consistent with the "steric-hyperlayer" model. Such systematic studies confirm the key role of size, density, and shape in the elution mode of RBCs in sedimentation FFF for living, micron-sized biological species. Using polymers as an analogy, the RBC population is described as highly "polydisperse". However, this definition must be reconsidered depending on the parameters under concern, leading to a matricial concept: multipolydispersity. It is observed that multipolydispersity modifications of a given RBC population are qualitatively correlated to the eluted sample band width.

Introduction

Field-flow fractionation (FFF) is a versatile family of separation techniques introduced in 1966 by J.C. Giddings (1). The general principle of these separation technologies is based on the coupling of a liquid (flowing in a laminar mode along a ribbon-like channel) with a field (applied perpendicularly to the great surface of the ribbon) (1–4). Very different applicable fields result in the versatility of this separation family. The fields can be thermal (5), electric (6), hydrodynamic (7,8), magnetic (9), or sedimentation (10) and lead to an increasing interest in biological applications (11–13). The sedimentation FFF that uses either mere earth gravity, known as gravitational FFF (GrFFF) (14–17), or centrifugal force, known as multigravitational FFF (SdFFF) (18–21), appears to be particularly well-suited for the purification, separation, and analysis of particles in the micron range (i.e., 2–30 µm in average diameter). The pioneering work of Caldwell et al. (12) in 1984 initiated the development of such a technique for cell separation. In particular, they showed that erythrocytes of different species were eluted in a size-dependent order (12). Sedimentation FFF methods were then used to study red blood cells (RBCs) of different origins and monitor experimental pathologies (22,23). It was also demonstrated that separations of biological interest, such as RBC age-dependent isolation, was possible (24), as well as the study of swelling resistance (25). Preliminary studies on nucleated cells of different origins were performed, and their elution characteristics were compared (12,13,26). The isolation of parasites, such as *Toxoplasma gondii* (27), *Trichomonas vaginalis* (28), *Trypanosomia* (29), and bacteria (30), was also successfully achieved. All these reports indicated that size and density played a key role in the elution of micron-sized cellular species. These indications were confirmed with organic particles, such as latex (14), and inorganic particles, such as silica beads (31), of different size. The effects of shape were also explored on biological material of submicron size (32) and on cellular material (12). These numerous experimental results led to the development of the so-called "steric-hyperlayer" elution mode of micron-sized particles in sedimentation FFF (4). In this elution mode, for particles of the same size, those of higher density were more retained (12,26). In the same manner but considering particles of identical density, those of greater size were eluted first.

* Author to whom correspondence should be addressed: e-mail cardot@unilim.fr.

By varying the cell medium and carrier phase osmolarity, RBC size, density, and shape are modified (33). Moreover, in hypoosmolar solutions, cell suspensions appear less polydisperse. Therefore, using carrier phases of different osmolarities with the same RBC population allows the description of their elution characteristics experimentally, depending on at least 2 cell parameters: volume and density. The values of these parameters are directly linked to the osmolarity of the medium if the cell membrane is considered to be a semipermeable one. Moreover, one specific feature of the human RBC (i.e., its plate shape in isotonic conditions) makes the analysis of the cell shape modifications possible. However, changes in the average size, density, and rigidity values affect the polydispersity of each parameter. A global analysis of polydispersity is possible by means of eluted population dispersion parameter (i.e., the height to equivalent theoretical plate) (HETP), leading to the concept of multipolydispersity.

Experimental

Theory

Osmosis phenomenon

Extensive descriptions of osmosis phenomenon have been published (34,35). Its consequences on RBC size and density can be formalized if the RBC membrane is supposed to ideally be semipermeable. In that case, in different osmolarity media, only pure water can flow through the membrane. Therefore, the cell volume can be calculated using the osmotic pressure definition (35). The RBC physical characteristic modifications in relation to the medium osmolarity ω (33) can be herein described by means of the following equations:

$$V = A - k\omega \qquad \text{Eq. 1}$$

$$D = B/(A - k\omega) \qquad \text{Eq. 2}$$

where V is the particle volume expressed in µm^3; D is its density; and A, B, and k are constants defined for human RBC with A = 168.4 µm^3, B = 104.5 µg, and k = 244.6 µm^3/Osm at 25°C (33).

Likewise, particle sphericity can be studied using the sphericity index (36), described as follows:

$$I = 4.84(V^{2/3})/S \qquad \text{Eq. 3}$$

where S is the membrane mean surface (estimated to be 140 µm^2 in isotonic conditions) (33). It was reported that I = 0.7 for normal RBC in isoosmolar solution (33). As RBC size increased in hypoosmolar media, the sphericity index increased up to a value of I = 1. In that situation, the particles become perfectly spherical without any change in the membrane surface (S). The RBC volume corresponding to a sphericity index of I = 1 using Equation 3 can be calculated at 155 µm^3. The medium osmolarity calculated by combining Equations 2 and 3 (for which RBC is totally spherical) is 170 mOsm. For osmolarity values lower than 170 mOsm, the particle is spherical. If osmolarity decreases, the cell membrane surface increases with evident consequences on density and volume.

RBC elution mode

It is now well established that in sedimentation FFF, most micron-sized species of biological origin elute according to a mechanism described as "steric-hyperlayer" (11,12). In such a mechanism, particles are focused into an equilibrium position in the channel thickness by the balance between the external field and opposite hydrodynamic lift forces. Because of the parabolic profile of the flow velocity, species in motion closer to the wall are more retained (11,12). The most important feature of this elution mode is the dependence of retention ratio to flow rate caused by the lift forces (3,4,12,13,37) whose specificities are not totally assessed to date. However, their influence and qualitative description have been investigated intensively (3,4,38,39). Previous experiments in SdFFF with RBCs have supported this elution mode (14,15,40,41). It was proved that in the steric-hyperlayer elution mode, cell characteristics such as density, size (28,26), or membrane rigidity (42) are involved, as are channel dimensions and flow characteristics (43). Therefore, cell modifications in size, density, and shape may lead to different elution positions in the channel thickness, leading to different elution characteristics whose results are described in this report.

FFF system

Three FFF systems were used for osmolarity-dependent RBC elutions. Two GrFFF (channels 1 and 2) systems, whose instrumental design has already been described (40), were used. The channel dimensions and system void volumes were 50 × 2 × 0.01 cm and 1.13 ± 0.07 mL (2 s, n = 5), respectively, for channel 1 and 50 × 2 × 0.025 cm, 2.52 ± 0.05 mL (2 s, n = 4), respectively, for channel 2. An SdFFF separator (channel 3), whose instrumental characteristics have already been reported (26), was also set up. Its rotor axis distance was 13.8 cm. The dimensions of channel 3 were 78.5 × 1 × 0.025 cm with a system void volume of 2.11 ± 0.09 mL (2 s, n = 4).

For all FFF experiments, a Gilson pump model 302 (Gilson Medical Electronics, Middletown, WI) connected to a pressure damper allowed flow rates ranging from 0.05 to 5 mL/min. A V 100L switching valve (Upchurch Scientific, Oak Harbour, WA) was used during the relaxation stage to divert the flow away from the channel for 4 min. Samples were introduced into the channel by means of a Rheodyne valve model 7125i (Rheodyne Incorporated, Cotati, CA) placed at the channel inlet. A Waters 440 photometer (Waters Corporation, Milford, MA) set at the channel outlet and operated at 365 nm allowed the detection of eluted particles. Signals were recorded on a Daewoo computer (Daewoo Europe, Roissy Charles de Gaulle, France) using a Soft 30160 card with lab-made software, allowing 16-byte precision, and operated at a frequency of 3 Hz.

FFF eluent

The eluents were phosphate buffer saline solutions (Biomerieux , Marcy-l'Etoile, France) of different osmolarities supplemented by 0.1% (w/w) bovine albumin (number A-4503, Sigma Chemical Company, St. Louis, MO). Eluents with osmolarities varying from 150 to 600 mOsm were prepared as follows: hypoosmolar solutions were made up from dilutions of an initial isoosmolar eluent, whereas hyperosmolar solutions were prepared using a reduced volume of sterile water (Biosedra Pharma,

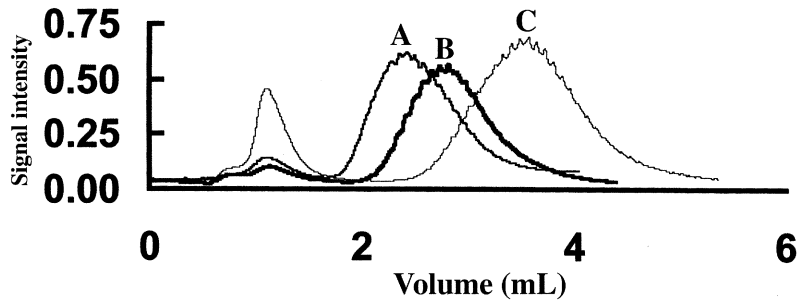

Figure 1. RBC fractograms in GrFFF: 200 mOsm hypoosmolar (A), 300 mOsm isoosmolar (B), 530 mOsm hyperosmolar (C). Conditions for channel 2: flow rate, 0.23 cm/s; stop-flow, 4 min; injection loop, 50 µL; red blood cells injected, 2.5 • 10^6; carrier phases, phosphate buffer saline solutions of different osmolarity supplemented with 0.2% (w/w) bovin albumin.

Louviers, France) for a given amount of phosphate buffer saline. The osmolarities were controlled using a Vapro vapour pressure osmometer model 5520 (Wescor, Logan, UT).

RBC samples

Blood was drawn from a healthy volunteer with his informed consent. Fresh samples were collected in sterile Vacutainer tubes (Becton Dickinson Vacutainer System, Meylan, France) containing potassium ethylene diamine tetracetic salt (K_3EDTA) as anticoagulant and refrigerated at 4°C. Within 2–3 days, the appropriate blood samples were diluted with the carrier phase 1 h prior to elution.

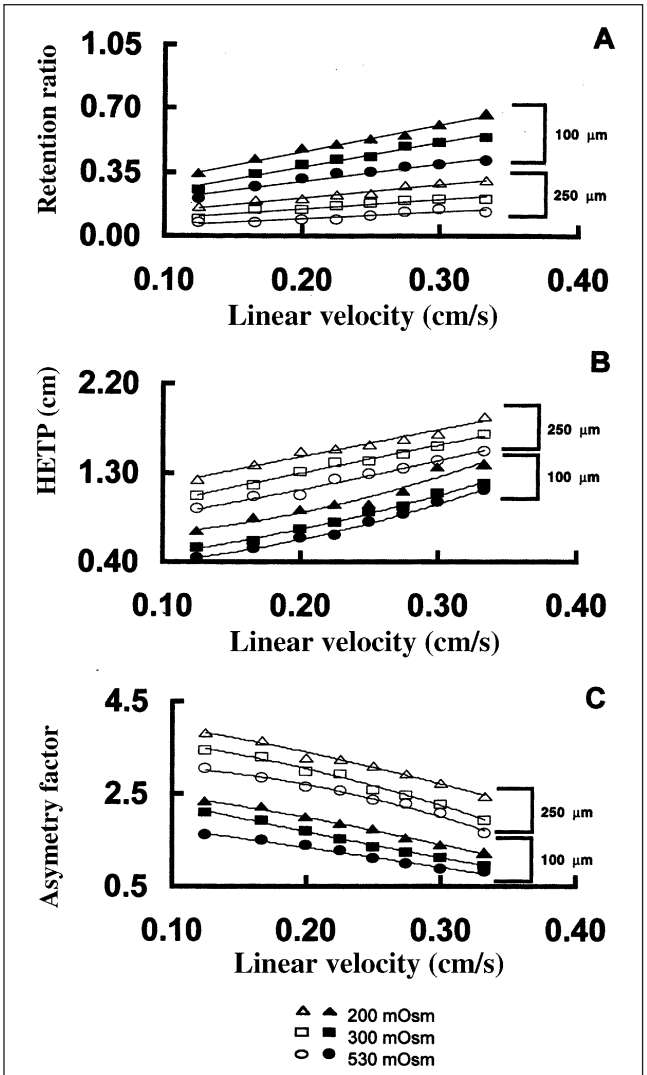

Figure 2. Effect of channel thickness on RBC elution: retention ratio (A), HETP (B), asymmetry factor (C). Conditions for channels 1 and 2: flow rate, ranged from 0 to 0.33 cm/s (0.13, 0.17, 0.20, 0.23, 0.25, 0.28, 0.30, 0.33); stop-flow, 4 min; 50-µL loop; red blood cells injected, 2.5 • 10^6; carrier phase, phosphate buffer saline solution (300 mOsm, pH 7.2) with 0.2% (w/w) bovine albumin.

Results and Discussion

Channel thickness

The steric-hyperlayer elution mode predicts that in a thin channel (≈ 100 µm), size is the dominant separation parameter (11,12). If the channel thickness increases, density differences will play an increased role (4,37,41,43).

Preliminary studies using GrFFF devices and fresh 100-fold diluted samples were performed with 2 channel thicknesses (100 µm and 250 µm). Typical signals obtained with channel 2 (fractograms) are shown in Figure 1. It is observed that RBCs diluted and eluted in a solution of reduced osmolarity (200 mOsm) were less retained. Such results are in accordance with the volume increase and the slight decrease in density of the RBC in the medium of reduced osmolarity. Peak parameters (retention ratio, asymmetry factor, HETP) were calculated according to the procedures published by Bidlingmeyer and Warren (44), and the data obtained are shown in Figure 2. As predicted (12,40), retention ratio increases to the flow rate increase. This increase is more intense in the thinner channel. The systematic increase of HETP with flow rate is linked to nonequilibrium elution characteristics, whatever limited role the injection procedure played as the sample was introduced in the vicinity of the accumulation wall. The thicker the channel, the larger the HETP, and in FFF for polydisperse particles, the wider the HETP, the more efficient the system can be (26). Therefore, channel 1 appears more efficient than channel 2. In any case, when the ratio of RBC size to channel thickness increased, HETP increased as described for other particles by Williams (3). The asymmetry factor is reduced as the flow rate increases and channel thickness decreases. Again, when comparing both channels, identical asymmetry factor values were associated with different flow and osmolarity conditions. Therefore, the use of SdFFF was chosen for an increased versatility provoked by the use of modular external field.

Injection procedures and FFF device

Since the early development of FFF techniques, 2 injection procedures have been described: flow and stop-flow modes (45). In the study of the appropriate injection procedure to monitor

RBC purification using channel 3, fresh 5-fold diluted blood samples were injected either directly into the established flow (flow injection) or while the flow was stopped for 4 min (stop-flow injection). Both procedures were tested at different flow velocities. Peak parameters were calculated, and the results are displayed in Figure 3. When the flow velocity increases, retention ratio and HETP increase and the asymmetry factor decreases, as shown in Figure 3. The decrease in the asymmetry factor was perhaps caused by a loss of resolution (HETP increase) when flow velocity increases. The differences observed between the 2 injection procedures decrease when the field increases or when the flow rate decreases. Although the samples are injected into the channel through the accumulation wall in this modified device, the RBCs were systematically more retained when using the stop-flow procedure, regardless of the flow rate and field intensity.

The extrapolated values of HETP for channel 3 at 0.30 cm/s are 2.21 ± 0.53, 1.13 ± 0.47 and 0.44 ± 0.21 for 3, 5, and 7 G, respectively. Then, at a given flow rate, channel 3 HETP values are in the same range as those of channel 1 (0.54 ± 0.17), particularly when the external field is increased (7 G). In addition, fractograms obtained from channel 3 appear to be more symmetrical (low asymmetry factor) than those of channel 1. Therefore, channel 3 can be considered at least as efficient as channel 1. Furthermore, channel 3 (multigravitational system) appeared more convenient because of the reduced time required to monitor RBC separation.

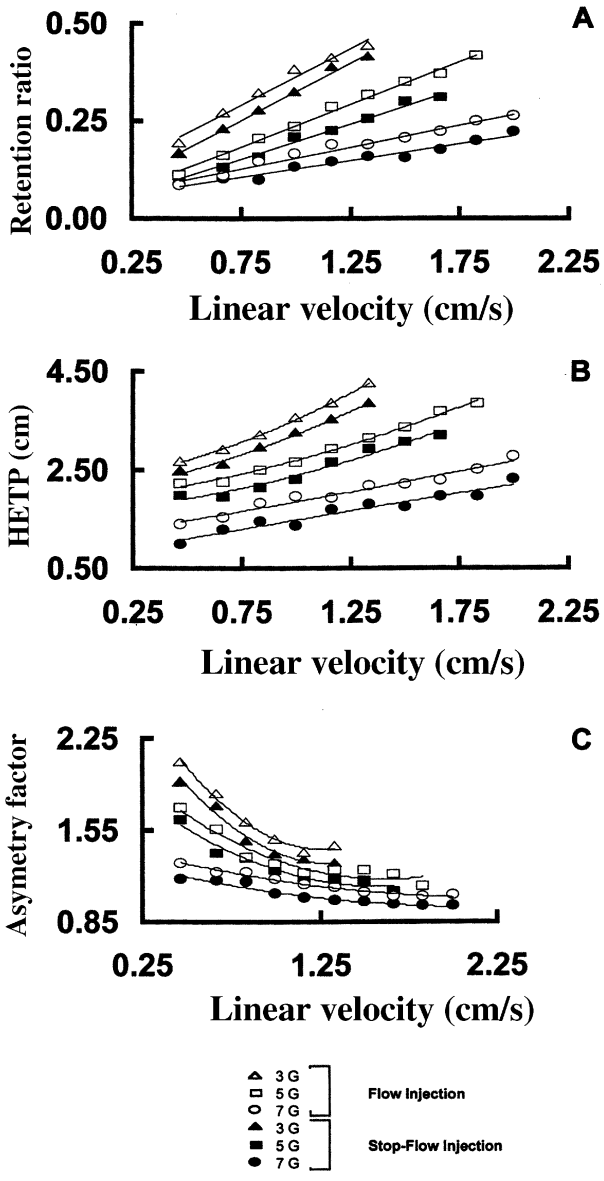

Figure 3. Effect of injection procedure on RBC fractogram characteristics: retention ratio (A), HETP (B), asymmetry factor (C). Conditions for channel 3: injection volume, 2.5 µL; flow rate, ranged from 0.47 to 2.00 cm/s (0.47, 0.67, 0.83, 1.00, 1.17, 1.33, 1.50, 1.67, 1.83, 2.00); carrier phase, phosphate buffer saline solution (300 mOsm, pH 7.2) with 0.2% (w/w) bovin albumin; stop-flow, 4 min.

RBC elution process

To determine the effects of the cells physical characteristics on their retention in FFF, experiments were performed using 7 solu-

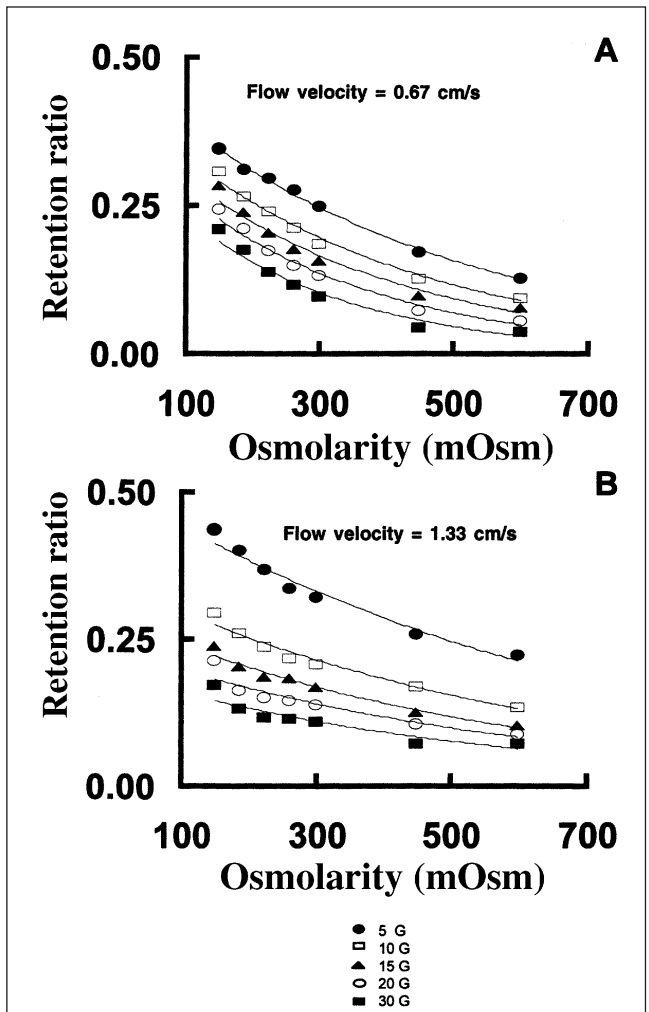

Figure 4. Effect of eluent osmolarity on RBC retention at 0.67 cm/s (A) and 1.33 cm/s (B). Conditions for channel 3: external field intensity, ranged from 5 to 30 G (5, 10, 15, 20, 30); stop-flow, 4 min; 2.5 µL loop; RBCs injected, 2.5 • 10^6; eluent osmolarity, ranged from 150 to 600 mOsm (150, 188, 225, 263, 300, 450, 600).

tions of different osmolarities as eluents: 4 hypoosmolar solutions (150, 172, 200, and 240 mOsm), 2 hyperosmolar carrier phases (400 and 600 mOsm), and an isoosmolar phase at 300 mOsm. Experiments were monitored at 5 field intensities (5, 10, 15, 20, 30 G) using the SdFFF system (i.e., channel 3). For each external field, 5 flow rates (0.47, 0.67, 1.00, 1.33, and 1.67 cm/s) were used. Retention ratios were calculated and plotted in Figure 4 for flow-velocities of 0.67 (Figure 4A) and 1.33 cm/s (Figure 4B). It can be observed in Figure 4 that the RBC retention ratio at a given flow rate and field intensity is osmolarity-dependent. The sphericity index calculated using Equations 1 and 3 showed that when the carrier phase osmolarity decreases, the RBC shape is modified from any shape in hyperosmolar solutions to a spherical shape in a solution of 150 mOsm. These results are in total accordance to those described 14 years ago by Caldwell et al.(12), who systematically studied retention properties of RBC in SdFFF. As RBC size decreases with the increase of the carrier phase osmolarity, the decrease in retention ratio observed is also in accordance with the steric-hyperlayer elution mode, which predicts qualitatively that in the equivalent conditions (field, flow-velocity, channel thickness), the hydrodynamically generated lifting force is higher for a particle of larger size. Such interpretation is complicated by the associated density decrease. Some reports analyzing the elution order of erythrocytes from different species have suggested that particle size is a major factor in determining the elution position (12,46). However, other studies evaluating samples from different individuals of the same species have acknowledged that size is not a major controlling factor (22,40). In the present study, a correlation between erythrocyte retention times and cell characteristics (i.e., size and density) is found, even if the part played by each parameter in the elution process is not evident. FFF elution characteristics of erythrocyte population appear to be controlled by several different cell characteristics, such as cell size and shape, cell density, membrane rigidity, and other features that are all contributing factors to a complex mechanism that determines the rate of retention through the FFF channel.

At a given medium osmolarity, the lift forces depend on the flow velocity and the external field, as shown in Figures 5 and 6, respectively. These results are in total accordance with the steric-hyperlayer elution mode (3,12,14). The retention ratio is systematically lower in hyperosmolar conditions when RBCs have a reduced volume and increased density.

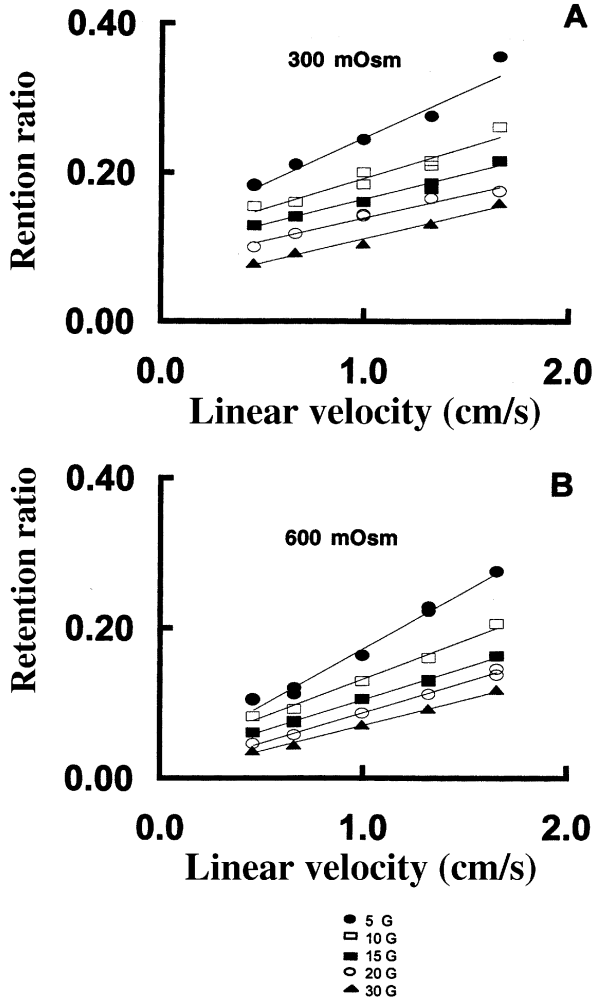

Figure 5. Effect of flow velocity on red blood cells retention at 300 mOsm (A) and 600 mOsm (B). Conditions for channel 3: external field intensity, ranged from 5 to 30 G; stop-flow, 4 min; 2.5 µL loop; RBCs injected, 2.5 • 10^6; flow rate, ranged from 0.47 to 1.67 cm/s (0.47, 0.67, 1.00, 1.33, 1.67).

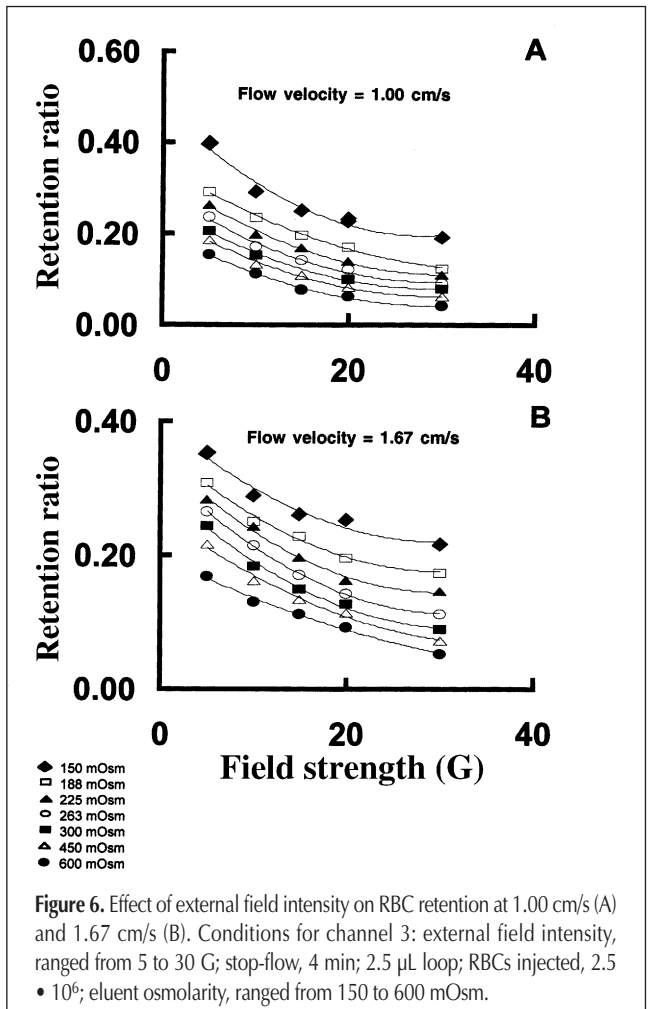

Figure 6. Effect of external field intensity on RBC retention at 1.00 cm/s (A) and 1.67 cm/s (B). Conditions for channel 3: external field intensity, ranged from 5 to 30 G; stop-flow, 4 min; 2.5 µL loop; RBCs injected, 2.5 • 10^6; eluent osmolarity, ranged from 150 to 600 mOsm.

The steric-hyperlayer focusing effect has been evidenced for nonbiological particles, such as latex beads (47), and for fixed RBCs (12). One of the major interests of this model in biology is that retention has been proved to depend on a large number of particle characteristics.

Efficiency

The channel efficiency described herein can be compared with those already published (12,26). The most interesting feature of the systematic study shown in Figure 3B is that under the same flow range conditions, RBC HETP values increase systematically when the flow rate increases. Calculated HETP values shown in Figure 3B are very similar to those found by Metreau et al. (26). Such results point out that living RBCs are more polydisperse in size, density, and shape (among others parameters) than fixed ones, as described by Caldwell et al. (12).

However, under the same retention conditions, such as the same retention ratio (that is the same sample average velocity), the higher HETP values for a polydisperse population may correspond to a secondary distribution of particles in the channel thickness due to slight differences in their physical parameters. In this case, polydisperse particles elute in thicker layers in the channel thickness than monodisperse ones. A question arose: will the medium osmolarity affect the RBC polydispersity?

HETP values can be linked to the polydispersity of a given sample population as described by Giddings et al. (48) and Karaiskakis et al. (49). HETP equations are now well-established and have been experimentally validated (49). Therefore, an osmolarity-dependent study of RBC polydispersity becomes possible. A given RBC sample is eluted at a given flow rate with media of different osmolarities, and the external field is chosen to obtain a given retention ratio. Experiments shown in Figure 7 were performed at 2 different average velocities and modified external field to obtain constant retention ratios of 0.20 and 0.25. At a given retention ratio, HETP increases with the carrier phase osmolarity value, suggesting strongly that the RBC population polydispersity was modified by the osmolarity of the medium. However, the polydispersity definition was set up for polymer analysis (49), and it is possible to reconsider the RBC population as a "multipolydisperse" one (that is, polydisperse in different directions, such as size, density, and shape). Therefore, the RBC population polydispersity can be described by a matrix of polydispersities (at least in size, shape, density) whose dimension definition can be complex. In the conditions described in this report, the medium osmolarity modifies the RBC population average characteristics and polydispersity. With decreased medium osmolarities, the sphericity index and cell volume of RBC increases, whereas the particle density decreases. Such a process modifies the average values. For example, in reduced osmolarity conditions, sphericity and volume average values are increased, and their polydispersity index is decreased, whereas that of density is increased. Therefore, the global HETP shows a reduced value. Using an analogy, the increase of HETP for high osmolarity can be explained. In terms of osmolarity, and because of the biophysical characteristics of the cell, 3 domains must be considered: the isoosmolar between 290 and 310 mOsm, the hypoosmolar above 310 mOsm, and the hyperosmolar below 290. In the isoosmolar region, the cell multipolydispersity matrix can be associated with a given HETP (i.e., 1.0–1.5 cm) as observed in Figure 7. This HETP value can be considered the global probe of the multipolydispersity of the cell in physiological conditions. On any side of the isoosmolar region, cell characteristics are modified. In hyperosmolar conditions, the cell's loss of water reduces its volume, increases its density, and modifies its shape. RBCs appeared as characteristic "echynocytes". It is highly difficult to discuss the polydispersity of the "echynocyte" shape, so only the volume and density polydispersity will be discussed.

Assuming the hypothesis that in isoosmolar conditions, RBC are associated with an average volume and density, and assuming that the density and volume polydispersity are given, some conclusions can be drawn from the curve characteristics of Figure 7. If the mean values of the parameters (e.g., size and density) decrease or increase, polydispersity index increases or decreases, respectively. This is what is observed when HETP values under hyperosmolar conditions are compared with isoosmolar ones. Under hyperosmolar conditions, the cell volume polydispersity increases, whereas its density polydispersity decreases. In the same manner, under hypoosmolar conditions, cell volume increases, reducing the volume polydispersity index as the density polydispersity increases. In hyperosmolar conditions, density seemed to play a major role, whereas in hypoosmolar conditions, size played the major role. This paradoxical situation is an image of some previous works that discussed the balance of the role played by size and density during FFF elutions (38,46). In light of the experimental situation described in Figure 7, there is some evidence that the polydispersity concept is not accurate enough. Its multidimensional extension that is the "multipolydispersity" matrix seemed essential for a mechanistic approach of the complex elution features of biological species. However, one can state that for a given species' average velocity in the FFF channel, cells are focused in a thinner "hyperlayer" in

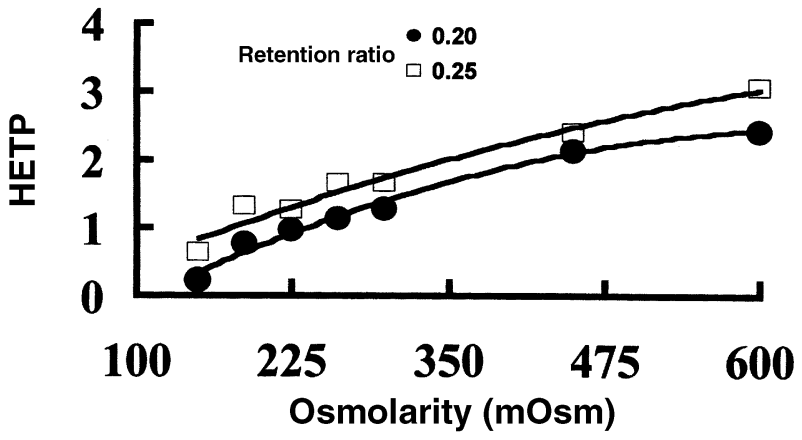

Figure 7. HETP evolution in function of flow osmolarity. Experimental conditions are the same as in Figure 5.

hypoosmolar conditions. This result strongly supports the global elution mechanism described by Giddings (50) and Caldwell et al. (12) as "steric-hyperlayer".

Conclusion

Whatever the sedimentation subtechnique used, the RBC elution profiles in different osmolar carrier phases showed analogous retention and band spreading properties. Retention increased systematically with osmolarity decrease, associated with the concomitant size increase and density decrease. Therefore, RBC osmolarity-dependent elution is mass dependent. Moreover, at a constant retention ratio that is equivalent to hydrodynamic conditions, RBC osmolarity band spreading increased with the increase of mass, size, and density polydispersity. Finally, in all the experimental conditions, the RBC osmolarity-dependent elution mode appeared to follow the RBC size- and density-dependent elution mode described as "steric-hyperlayer". Specific size-dependent and carrier-flow-rate independent elution modes described as "steric" were not experimentally observed under the experimental conditions described herein. The results described in this report generated basic rules to build an empirical elution model in SdFFF based on the balanced effects of size, density, mass, shape, and rigidity of the RBC. To assess the specific effects of these parameters and osmolarity-dependent size, shape, mass, density, and rigidity, average and polydispersity models must be set up whose basic hypothesis is as follows: the RBC membrane is a pure semipermeable one, and no RBC components (out of pure water) are released or integrated during the osmolar shock. If these conditions are fulfilled, it is possible by means of bibliographic data to evaluate average and polydispersity values of the volume, density, and consequently the mass of RBC, as well as the sphericity and rigidity. Purely empirical chemometric techniques based on these models will allow the discrimination of the relative effects of these parameters on the RBC osmolarity-dependent elution.

Acknowledgments

J.M. Marbouty, head of the Department of English for Specific Purpose, College of Pharmacy, Limoges University, is acknowledged for English language corrections.

References

1. J.C. Giddings. A new separation concept based on a coupling of concentration and flow nonuniformities. *Sep. Sci.* **1:** 123–25 (1966).
2. P.S. Williams and J.C. Giddings. Power programmed field flow fractionation: a new program form for improved uniformity in fractionating power. *Anal. Chem.* **59:** 2038–44 (1987).
3. P.S. Williams, T. Koch, and J.C. Giddings. Characterisation of near-wall hydrodynamic lift forces using sedimentation field flow fractionation. *Chem. Eng. Commun.* **111:** 121–47 (1992).
4. J.C. Giddings. Field-flow fractionation: separation and characterisation of macromolecular-colloidal-particulate materials. *Science* **260:** 1456–65 (1993).
5. G. Liu and J.C. Giddings. Separation of particles in aqueous suspensions by thermal field-flow fractionation: measurement of thermal diffusion coefficients. *Chromatographia* **34:** 483–92 (1992).
6. K.D. Caldwell, L.F. Kesner, M.N. Myers, and J.C. Giddings. Electrical field-flow fractionation of proteins. *Science* **176:** 296–98 (1972).
7. S.K. Ratanathanawongs, I. Lee, and J.C. Giddings. Separation and characterisation of 0.01–50 µm particles using field-flow fractionation. *Am. Chem. Soc. Symp. Ser.* **472:** 229–34 (1991).
8. K.G. Wahlund and A. Litzen. Application of an asymmetric flow field-flow fractionation channel to the separation and characterisation of proteins, plasmid fragments, polysaccharides and unicellular algae. *J. Chromatogr.* **461:** 73–87 (1989).
9. J. Janca. Field-flow fractionation in biopolymers analysis. *Trends Anal. Chem.* **2:** 278–81 (1983).
10. J.C. Giddings. Field-flow fractionation. *Chem. Eng. News* **66:** 34–45 (1988).
11. L.E. Schallinger, W.W. Yau, and J.J. Kirkland. Sedimentation field-flow fractionation of DNA's. *Science* **225:** 434–37 (1984).
12. K.D. Caldwell, Z.-Q. Cheng, P. Hradecky, and J.C. Giddings. Separation of human and animal cells by steric field-flow fractionation. *Cell Biophys.* **6:** 233–51 (1984).
13. S. Hoffstetter-Kuhn, T. Rosler, M. Ehrat, and H.M. Widmer. Characterisation of yeast cultivations by steric sedimentation field-flow fractionation. *Anal. Biochem.* **206:** 300–308 (1992).
14. J. Pazourek and J. Chmelik. Optimization of the separation of micron-sized latex particles by gravitational field-flow fractionation. *Chromatographia* **35:** 591–96 (1993).
15. J. Plocek, P. Konecny, and J. Chmelik. Modification of glass channel walls for separation of biological particles by gravitational field-flow fractionation. *J. Chromatogr. B* **656:** 427–31 (1994).
16. C. Bories, P.J.P. Cardot, V. Abramowski, C. Pous, A. Merino-Dugay, and B. Baron. Elution mode of *Pneumocystis carinii* cysts in gravitational field-flow fractionation. *J. Chromatogr.* **579:** 143–52 (1992).
17. V. Yue, R. Kowal, L. Neargarder, L. Bond, A. Muetterties, and R. Parsons. Miniature field-flow fractionation system for analysis of blood cells. *Clin. Chem.* **40:** 1610–14 (1994).
18. K.D. Caldwell, T.T. Nguyen, J.C. Giddings, and H.M. Mazzone. Field-flow fractionation of alkali liberated polyhedrosis virus from gypsy moth. *J. Virol. Methods* **1:** 241–56 (1980).
19. S.M. Mozersky, K.D. Caldwell, S.B. Jones, B.E. Maleeff, and R.A. Barford. Sedimentation field-flow fractionation of mitochondrial and microsomal membranes from corn roots. *Anal. Biochem.* **172:** 113–23 (1988).
20. K.D. Caldwell, B.J. Compton, J.C. Giddings, and R.J. Olson. Sedimentation field-flow fractionation: a method for studying particulates in cataractous lens. *Invest. Ophtamol. Visual Sci.* **25:** 153–59 (1984).
21. T. Sklaviadis, R. Dreyer, and L. Manuelidis. Analysis of Creutzfeldt-Jakob disease infectious fractions by gel permeation chromatography and sedimentation field-flow fractionation. *Virus Res.* **26:** 241–54 (1992).
22. A. Merino-Dugay, P.J.P. Cardot, M. Czok, M. Guernet, and J.P. Andreux. Monitoring of an experimental red blood cells pathology with gravitational field-flow fractionation. *J. Chromatogr.* **579:** 73–83 (1992).
23. J.P. Andreux, A. Merino, M. Renard, F. Forestier, and P.J.P. Cardot. Separation of red blood cells by gravitational field-flow fractionation. *Experim. Hemat.* **21:** 326–30 (1993).
24. P.J.P. Cardot, J.M. Launay, and M. Martin. Age-dependent elution of human red blood cells in gravitational field flow fractionation. *J. Liq. Chromatogr.* **20:** 2543–53 (1997).
25. K.D. Caldwell. Personal communication.
26. J.M. Metreau, S. Gallet, P.J.P. Cardot, V. Le Maire, F. Dumas, A. Hernvann, and S. Loric. Sedimentation field-flow fractionation of

cellular species. *Anal. Biochem.* **251:** 178–86 (1997).
27. F. Bouamrane, N.E. Assidjo, B. Bouteille, M.F. Dreyfuss, M.L. Darde, and P.J.P. Cardot. Sedimentation field-flow fractionation to *Toxoplasma gondii* separation and purification. *Submitted to J. Pharm. Biomed. Anal.*
28. A. Bernard, C. Bories, P.M. Loiseau, and P.J.P. Cardot. Selective elution and purification of living *Trichomonas vaginalis* using gravitational field-flow fractionation. *J. Chromatogr.* **664:** 444–48 (1995).
29. S. Gallet, J.M. Metreau, P. Loiseau, C. Bories, and P.J.P. Cardot. Isolation of bloodstream trypanosomes by sedimentation field-flow fractionation. *J. Microcol. Sep.* **9:** 253–59 (1997).
30. A. Fox, L.E. Schallinger, and J.J. Kirkland. Sedimentation field-flow fractionation of bacterial cell wall fragments. *J. Microbiol. Methods* **3:** 273–81 (1985).
31. P. Reschiglian and G. Torsi. Determination of particle size distribution by gravitational field-flow fractionation. *Chromatographia* **40:** 467–73 (1995).
32. J.J. Kirkland, L.E. Schallinger, and W.W. Yau. Effect of particle conformation on retention in sedimentation field-flow fractionation. *Anal. Chem.* **57:** 2271–75 (1985).
33. R.S. Weinstein. In *The Red Blood Cell*, Vol. 1, 2nd ed., D.N. Surgenor, Ed. Academic Press, New York, NY, 1974.
34. M. Magnani, L. Rossi, M. D'ascenzo, I. Panzani, L. Bigi, and A. Zanella. Erythrocyte engineering for drug delivery and targeting. *Biotechnol. Appl. Biochem.* **28:** 1–6 (1998).
35. M. Rasia and A. Bollini. Red blood cell shape as a function of medium's ionic strength and pH. *Biochim. Biophys. Acta.* **1372:** 198–204 (1998).
36. M.D. Delano. Simple physical constraints in hemolysis. *J. Theor. Biol.* **175:** 517–24 (1995).
37. J.J. Kirkland and W.W. Yau. Simultaneous determination of particle size and density by sedimentation field-flow fractionation. *Anal. Chem.* **55:** 2165–70 (1983).
38. J.C. Giddings, G. Karaiskakis, and K.D. Caldwell. Density and particle size of colloidal material measured by carrier density variations in sedimentation field-flow fractionation. *Sep. Sci. Technol.* **16:** 607–618 (1981).
39. P.J.P. Cardot, C. Elgea, M. Guernet, D. Godet, and J.P. Andreux. Size- and density-dependent elution of normal and pathological red blood cells by gravitational field-flow fractionation. *J. Chromatogr.* **654:** 193–203 (1994).
40. A. Bernard, B. Paulet, V. Colin, and P.J.P. Cardot. Red blood cell separations by gravitational field-flow fractionation: instrumentation and applications. *TRAC.* **14:** 266–73 (1992).
41. E. Assidjo and P.J.P. Cardot. Sedimentation field-flow fractionation at gravitational field of red blood cells: systematic studies of injection conditions. *J. Liq. Chromatogr.* **20:** 2579–97 (1997).
42. X. Tong and K.D. Caldwell. Separation and characterization of red blood cells with different membrane deformability using steric field-flow fractionation. *J. Chromatgr. B* **674:** 39–47 (1995).
43. J.C. Giddings. Measuring colloidal and macromolecular properties by FFF. *Anal. Chem.* **67:** 592A–598A (1995).
44. B.A. Bidlingmeyer and F.V. Warren, Jr. Column efficiency measurement. *Anal. Chem.* **56:** 1583A–1587A (1984).
45. J.C. Giddings and M.N. Myers. Steric field-flow fractionation: a new method for separating 1–100 µm particles. *Sep. Sci. Technol.* **13:** 637–45 (1978).
46. B.N. Barman, E.R. Ashwood, and J.C. Giddings. Separation and size distribution of red blood cells of diverse size, shape and origin by flow/hyperlayer field-flow fractionation. *Anal. Biochem.* **212:** 35–42 (1993).
47. H.K. Jones, B.N. Barman, and J.C. Giddings. Resolution of colloidal latex aggregates by sedimentation field-flow fractionation. *J. Chromatogr.* **455:** 1–15 (1988).
48. J.C. Giddings, F.J.F. Yang, and M.N. Myers. Sedimentation field flow fractionation. *Anal. Chem.* **46:** 1917–24 (1974).
49. G. Karaiskakis, A. Koliadima, and K. Klepernik. Estimation of polydispersity in polymers and colloids by hyperlayer field flow fractionation. *Colloid. Polym. Sci.* **269:** 583–89 (1991).
50. J.C. Giddings. Hyperlayer field flow fractionation. *Sep. Sci. Technol.* **18:** 765–73 (1983).

Manuscript accepted May 28, 1999